

---

# FSL-Rectifier: Rectify Outliers in Few-Shot Learning via Test-Time Augmentation

---

Yunwei Bai   Ying Kiat Tan   Tsuhan Chen  
National University of Singapore

## Abstract

Few-shot-learning (FSL) commonly requires a model to identify images (queries) that belong to classes unseen during training, based on a few labelled samples of the new classes (support set) as reference. As the test classes are novel, FSL is challenging with high generalization error with respect to the novel classes, where outliers query or support image during inference exacerbate the error further. So far, plenty of algorithms involve training data augmentation to improve the generalization capability of FSL models. In contrast, inspired by the fact that test samples are more relevant to the target domain, we believe that test-time augmentation may be more useful than training augmentation for FSL. In this work, to reduce the bias caused by unconventional test samples, we generate new test samples through combining them with similar train-class samples. Averaged representations of the test-time augmentation are then considered for few-shot classification. According to our experiments, by augmenting the support set and query with a few additional generated sample, we can achieve improvement for trained FSL models. Importantly, our method is universally compatible with different off-the-shelf FSL models, whose performance can be improved without extra dataset nor further training of the models themselves. Codes are available at <https://github.com/WendyBaiYunwei/FSL-Rectifier>.

## 1 Introduction

While deep learning has gained much success in practical contexts, deep neural networks (DNN) are data hungry, and the high expense of label collection remains a pain point [14, 32, 33, 36]. Furthermore, some classes of data can be rare and difficult to collect. For example, in facial expression recognition, class imbalance problems are prevalent, as facial expressions like happy smile abound, but expressions like disgust are relatively few [1]. Few-Shot Learning (FSL) tackles classification problems with limited test-class labels [32]. It is commonly assumed that FSL models have to classify novel-class images when presented with a *support set* comprising only a few shots of labeled samples as reference [32]. While the data constraint is practically meaningful, the access to labelled data poses generalization challenges to FSL models, most of which are DNN [32]. Such a generalization error mainly involves the generalization gap between the training data and the test data, which can be exacerbated by unconventionality of test data samples [9, 23, 32].

So far, different algorithms are proposed to tackle the issue of high generalization errors. Most of works involve training augmentation for enhancing the generalization capacity of FSL models [4, 5, 15, 22, 26, 31]. However, such augmentation involves model training over an increased amount of data, costing extra computation resources over every additional FSL model trained. Furthermore, augmentation over the training dataset can still be limited in performance, since the gap between the testing data and the augmented training data remains wide.

In this work, we propose to tackle FSL via test-time augmentation instead of training-time augmentation. Our method is named *FSL-Rectifier*, which essentially combines each test sample with its

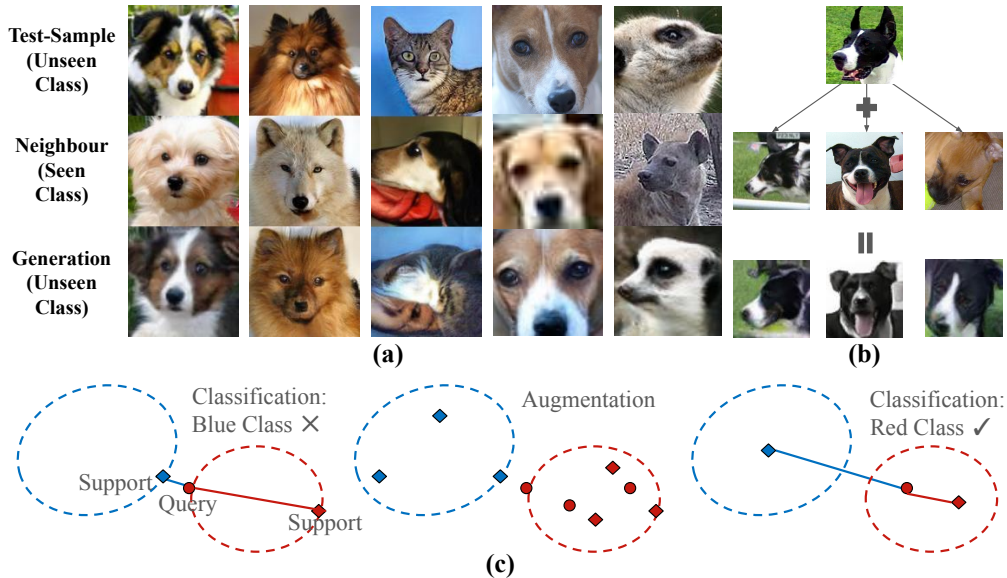


Figure 1: Illustration of our key idea and motivation. (a): The first image in each column of the animals dataset is the original test sample, the second is neighbour sample from the test class. The last image is the generation based on style of original test sample and shape of neighbour. (b): Given different neighbour samples, each test sample can be augmented to become multiple copies. (c): How averaged augmentations may correct wrong classifications.

similar training-set samples. To achieve the combination, we have three main components: 1) *image combiner*, 2) *neighbour selector* and 3) *augmenter*. For the image combiner, we train a generative image translator model over the training classes. The image combiner takes in two images, combining the shape (e.g. animal pose and position of eyes) of one image and the style (e.g. animal fur style) of another via an adversarial auto-encoder [12]. The combination is illustrated in a) of Figure 1. The discriminator of the adversarial auto-encoder can discriminate quality of the synthesized images, and are then used as our neighbour selector. During testing of any off-the-shelf FSL models, a few train-class images are randomly sampled. The neighbour selector can select a better candidate to be combined with a test-class sample. This sample can either be a query to be classified, or a support set sample used as the reference for few-shot classification. Finally, we average representations of augmented copies and the original test samples. The augmentation is illustrated in b) of Figure 1. Via this approach, we can make the averaged representations closer to their centroids, correcting biased predictions of an existing FSL model, as illustrated in c) of Figure 1.

Our design has two main benefits. Firstly, the combined samples tend to form a more typical and robust representation compared to a single sample, which may have been an outlier. Secondly, our method is test-time-only. The training of the image translator and the neighbour selector is associated with a dataset instead of any individual FSL model. Therefore, this method can become uniquely advantageous compared to train-class augmentation if minimal training of FSL models is desirable. To summarize, We design a test-time augmentation method for FSL models via generative adversarial auto-encoder. To our best knowledge, we are also the first work that proposes test-time augmentation via generative techniques for FSL.

## 2 Related Works

**Few-shot learning** sees pioneer works from [3], which formulate a bayesian learning framework to quickly adapt to novel classes. For a broader field of few-shot learning, mainstream algorithms include the meta-learning methodology and metric-learning methodology [19, 24, 32]. Related to our works, FSL algorithms include the Matching Network [27] and the Prototypical Network (ProtoNet) [23], which measure the euclidean distance (or cosine similarity) between query and support embeddings for identifying the most probable categories of the queries. Similar algorithms include FEAT [35], which incorporates a transformative layer (i.e. self-attention [25]) layer to the

Matching Network set-up, enhancing the expressiveness of image embeddings. ProtoNet and FEAT are adopted in our experiments.

**Image translation** is a form of generative technique. Deep generative models involve popular architectures like the Variational Auto-Encoder (VAE) and the Generative Adversarial Network (GAN) [16, 29], while the Adversarial Auto-Encoder combines VAE and GAN. Celebrated image translation models include the CycleGAN [37], which merges two pictures through a symmetric pair of GAN networks. Other related works such as the StyleGAN [8], Coco-Funit/Funit [13, 21] and more [17, 30] can also achieve realistic results in generating new images conditioned on different user requirements. Some image translation works like [8, 13] adopt style transfer technique AdaIN [7], which applies arbitrary styles to existing images via aligning the distribution of their latent-level features to those of the style images.

**Data augmentation for FSL** efforts are mostly centered on training data augmentation. Earlier, a “congealing” method grafts variations from similar training classes to a separate training class [32]. Similar ideas are also seen in FSL works like [4, 5, 15, 22, 26, 31], where the authors aim to augment the training dataset to achieve better generalization among FSL models. A work similar to ours is [9], where the authors correct the angles of traffic signs through VAE and logo prototype images. While most of the prior works focus on training-phase augmentation, we only focus on testing-phase augmentation for models that are already trained. Additionally, in the field of test-time augmentation, only a few works apply the test-time augmentation techniques to FSL [10, 34]. These authors observe improvement for FSL model performance through traditional image augmentation transformations like cropping and resizing. In comparison to the prior works, our work combines both training data and the testing data, instead of just focusing on either of these two splits separately.

### 3 FSL-Rectifier

#### 3.1 Problem Formulation

Commonly, FSL classification tasks follow an  $N$ -way- $K$ -shot set-up;  $N$  represents the number of classes being classified and  $K$  denotes the number of labeled samples per class. These  $K \times N$  samples, denoted as  $S = \{x_1^{(1)}, x_2^{(1)}, \dots, x_{K-1}^{(N)}, x_K^{(N)}\}$ , are the *support set*. Consider an FSL classifier  $h$ .  $h$  learns from training classes  $C^b$  with complete supervision, and is then tested on a set of test classes  $C^n$ . The training classes and test classes do not overlap (i.e.  $C^b \cap C^n = \emptyset$ ). Meanwhile, the test classes contain just a few labeled samples. These labeled samples serve as the support set  $S$  during testing of  $h$  [2, 23, 24, 32, 35]. During *training*, the classifier  $h$  is presented with a labelled support set comprising samples from  $N$  classes, and queries  $q$  sub-sampled from the  $N$  classes.  $h$  has to learn or predict which categories  $q$  belong to by referring to  $S$ . The  $N$  classes are a subset of training classes  $C^b$ . During *testing*,  $h$  has to predict classes of  $q$  based on labels of  $S$ , where both  $q$  and  $S$  are sampled from  $C^n$  [2, 23, 24, 32, 35].

#### 3.2 Overall Pipeline

As illustrated in Figure 2, our method, FSL-Rectifier, consists of three main components: a) image combiner, b) neighbour selector, and c) augmentor. At stage 1, our goal is to train a generative image combiner that takes in a training sample and a test sample, producing a test-class sample based on the pose of training sample. At stage 2, our goal is to train a neighbour selector, which takes in a test sample and a set of candidate training samples, returning a suitable training sample to be combined with the test sample. The suitable sample is termed *neighbour*. At stage 3, we perform test-time augmentation. For each test sample, we pick its neighbours via the neighbour selector. Then, we produce generated test samples based on the neighbours and original test sample. For FSL classification, we consider the average image embeddings of original test samples and generated test samples, instead of just the single original sample.

#### 3.3 Method

**Image Combiner.** Our aim is to generate new test-class samples without seeing other test samples, while employing training-sample information which a trained FSL model is familiar with. Therefore,

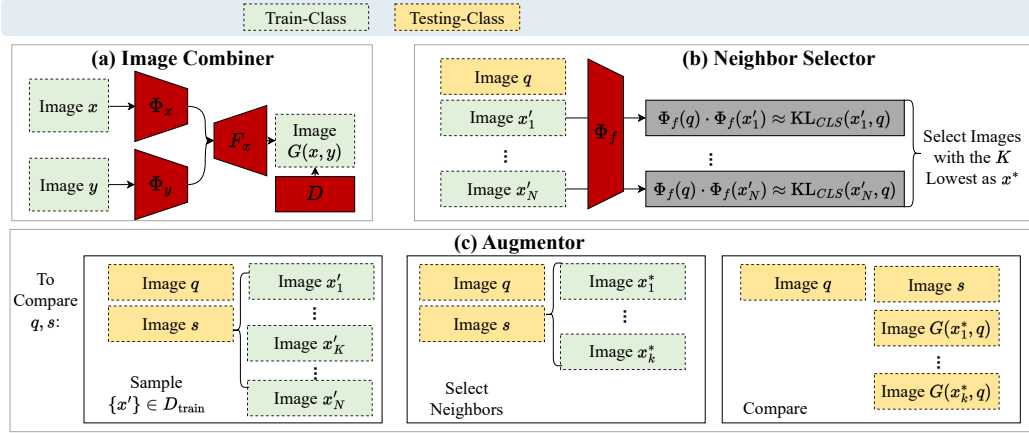


Figure 2: Architecture of FSL-Rectifier.

the objective of the image combiner is to combine information from both the test class  $C^n$  and the training class  $C^b$ , translating an input train-class sample to a test-class sample.

Let  $x$  denote the image from which we extract the shape or pose. Let  $y$  denote an image from which we extract the class-defining style. The image combiner  $G$  consists of a shape encoder  $\Phi_x$ , a style encoder  $\Phi_y$  and a decoder  $F_x$ . The style encoder captures the style and appearance of an image, and the shape encoder captures the pose and shape of another image. The image combiner essentially produces images  $G(x, y) = F_x(\Phi_x(x), \Phi_y(y))$ .

During training, we solve the following minimax optimization problem:

$$\min_D \max_G \mathcal{L}_{\text{GAN}}(D, G) + k_R \mathcal{L}_R(G) + k_{\text{FM}} \mathcal{L}_{\text{FM}}(G). \quad (1)$$

where  $D$  is the discriminator in the GAN network,  $k_R$  and  $k_{\text{FM}}$  are hyperparameters,  $\mathcal{L}_{\text{GAN}}$  is the GAN-loss,  $\mathcal{L}_R$  is the reconstruction loss and  $\mathcal{L}_{\text{FM}}$  is the feature matching loss. We introduce each loss below.

Firstly, the GAN-loss drives the training of both the generator and the discriminator to compete through the following objective function:

$$\mathcal{L}_{\text{GAN}}(D, G) = \mathbb{E}_x[-\log D(x)] + \mathbb{E}_{x,y}[\log(1 - D(G(x, y)))] \quad (2)$$

Here, the discriminator tries to discern between real and images produced by the generator, while encouraging the generation to become the same class as the original test sample class through a classifier  $h_d$  coupled with the discriminator encoder  $\Phi_d$ , where  $D = \Phi_d \circ h_d$ .  $h_d$  is a fully connected layer with output size equal to the number of training classes. At the same time, the generator tries to fool the discriminator.

The reconstruction loss  $\mathcal{L}_R$  helps generator  $G$  generate outputs that resemble the shape of the target images, which are designed as the input images themselves in the loss function:

$$\mathcal{L}_R(G) = \mathbb{E}_x[\|x - G(x, x)\|_1]. \quad (3)$$

The feature matching loss helps regularize the training, generating new samples that possess the style of the image  $y$ :

$$\mathcal{L}_{\text{FM}}(G) = \mathbb{E}_{x,y}[\|\Phi_d(G(x, y)) - \Phi_d(y)\|_1]. \quad (4)$$

Here,  $\Phi_d$  is the feature extractor, which is obtained from removing the last layer (the classifier layer  $h_d$ ) from discriminator  $D$ .

The shape encoder  $\Phi_x$  is made of convolutional layers and residual blocks, converting input images to their latent representations. The style encoder  $\Phi_y$  consists of convolutional layers. The decoder  $F$  consists of a few adaptive instance normalization (AdaIN) residual blocks [7] followed by upscaling using convolutional layers [12]. This image combiner, including the reconstruction loss and feature matching loss, follow prior techniques [11, 12, 17, 21, 30]. Lastly, during training of the image combiner, we only use the train-split of a dataset, leaving the test-split dataset unseen.

**Neighbour Selector.** Image combiner  $G$  as a generative model can at times produce poor results. Furthermore, it can be fallacious to presume that features among different classes can always be mix-and-matched in meaningful ways. To ensure that the good-quality generations are used during the testing phase, we design the neighbour selector which, when presented with a pool of candidate neighbour images, can return the better candidates for the generation of new test samples. Intuitively, a naive way to implement this neighbour selector is to generate new test samples based on each neighbour candidate, before selecting the best generated sample based on a measure of generation quality [28]. However, it can be computationally expensive to generate all these images and then assess their quality individually. Therefore, our goal is to learn a representation space (i.e. image encoder in this context) which indicates whether two images, when their features get multiplied, can produce quality generation. Essentially, we aim to generate samples that belong to the test class while skipping the actual generation.

We train a neighbour selector using randomly sampled datapoints from both the training set, which is denoted as  $\mathcal{D}_{\text{train}}$  consisting of samples from  $C^b$ , and the testing set,  $\mathcal{D}_{\text{test}}$  consisting of samples from  $C^n$ , without any supervision information. Reusing the trained image combiner, we aim to update the discriminator encoder  $\Phi_d$  to become  $\Phi_f$  such that, for a pair of original test sample  $y \in \mathcal{D}_{\text{test}}$  and neighbour  $x \in \mathcal{D}_{\text{train}}$ ,  $\Phi_f(x) \cdot \Phi_f(y)$  returns a ‘‘generation quality’’ score, which estimates the quality of generation for  $G(x, y)$ . To achieve this, during training of  $\Phi_f$ , we feed combinations of test samples and neighbour candidates  $\{x, y\}$  and minimize the following objective function  $\mathcal{L}_{KL}$ , defined by:

$$\mathbb{E}_{x,y} [\|\Phi_f(x) \cdot \Phi_f(y) - KL(\sigma(h_d(G(x, y))) \parallel \sigma(h_d(x)))\|_1]. \quad (5)$$

Here,  $\sigma$  is the softmax function,  $h_d(\cdot)$  represents the logits output from the trained and frozen classifier  $h_d$  in discriminator  $D$ .

During training of the neighbour selector, we minimize the difference between training sample and test sample feature product  $\Phi_f(x) \cdot \Phi_f(y)$ , and the KL divergence between their respective class logits returned by the discriminator,  $KL(\sigma(h_d(G(x, y))) \parallel \sigma(h_d(x)))$ . In other words, we obtain an encoder which produces train-test features that, when multiplied in a pairwise manner, indicate the degree of class difference between the generation and original test sample. When the degree of difference is small, the generation is desirable. Therefore, during actual testing, a candidate neighbour sample  $x^*$ , whose feature leading to the lowest divergence score when multiplied with the original test sample feature  $\Phi_f(y)$ , is selected from a pool of neighbour candidates  $\{x'\}$ :

$$x^* = \underset{x'}{\operatorname{argmin}} \Phi_f(x') \cdot \Phi_f(y). \quad (6)$$

As seen in Equation 6, we can eliminate the generation of actual new test samples. Meanwhile, the same configuration for the image combiner is used. We finetune the neighbour selector  $D$  based on existing model parameters learnt from stage 1, keeping the training for neighbour selector simplistic.

**Augmentor.** Suppose we generate  $k$  new samples for  $n$ -way-1-shot classification.  $h = h' \circ \Phi$  is the trained FSL model with encoder  $\Phi$  and classifier  $h'$ . The feature averaging  $R_k(y)$  is a function which translates one image sample  $y$  to  $k$  copies of generated images, before considering their average embeddings. The function can be defined as below:

$$R_k : y \rightarrow \frac{1}{k+1} \sum \{\Phi(G(y, x_1^*)), \dots, \Phi(G(y, x_k^*)) + \Phi(G(y, y))\}. \quad (7)$$

where  $y$  is the test sample,  $\{x_i^*\}$  are neighbours. Note that one can tune embedding weights during the embedding summation. Final FSL predictions can be rendered based on  $h'$ , or the classifier of  $h$ :

$$\hat{y} = h'(R_k(q) | \{R_k(s_1), \dots, R_k(s_n)\}). \quad (8)$$

where  $q$  represents the query image and  $s$  represents each support set image.

## 4 Implementation and Experiments

### 4.1 Datasets

In this work, we use the Animals dataset, which is sampled from the ImageNet dataset [20]. The Animals dataset contains carnivorous animal images [12]. The Animals dataset train-test split follows prior works [12]. All images from these datasets are colored and resized to  $84 \times 84$  dimension during training and testing of FSL models.

	Euclidean Distance (%)		Cosine Similarity (%)	
	ProtoNet-Conv4	FEAT-Conv4	ProtoNet-Conv4	FEAT-Conv4
1-Shot + 1-Query	54.64 ± 0.60	46.86 ± 0.59	56.72 ± 0.60	46.80 ± 0.59
4-Shot + 4-Query (Oracle)	80.20 ± 0.56	69.96 ± 0.57	79.74 ± 0.56	69.92 ± 0.57
Rotate	53.68 ± 0.60	50.60 ± 0.59	54.68 ± 0.60	50.36 ± 0.59
ColorJitter	52.25 ± 0.60	46.71 ± 0.58	52.24 ± 0.60	46.64 ± 0.58
Affine	52.25 ± 0.60	46.07 ± 0.60	49.68 ± 0.60	46.68 ± 0.60
Mix-Up	54.44 ± 0.63	52.20 ± 0.59	54.60 ± 0.63	47.76 ± 0.59
<b>FSL-Rectifier (Ours)</b>	<b>57.90 ± 0.79</b>	<b>53.28 ± 0.56</b>	<b>57.38 ± 0.79</b>	<b>52.80 ± 0.56</b>

Table 1: Animals 5-way-1-shot accuracy.

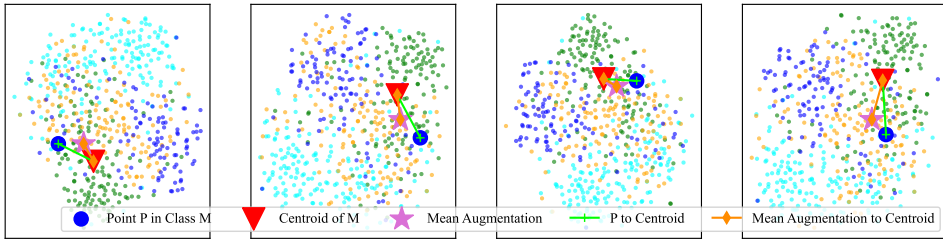


Figure 3: TSNE plot indicating that average augmentation of a random point P (★) stay closer to the class centroid (▼), compared to the random point P (●) on its own. Best viewed in colors.

## 4.2 Models

To obtain trained FSL models used in this work, we use the ProtoNet [23], the FEAT, and the DeepSet [35] with either a euclidean-distance or cosine-similarity classifier for experiments. Our experiments pair the algorithms with both Conv4 and Res12 [6] encoders, which we adopt from [35]. We conduct pretraining of both of these encoders before training them further on different FSL algorithms. For the training of Animals FSL models, we set the training epochs to 50, the learning rate to  $1 \times 10^{-4}$  for Conv4-based models and  $2 \times 10^{-4}$  for Res12-based models. For training of the GAN-based image image combiner, we follow implementations mainly from [12]. We set the maximum training iteration to 100,000, batch size to 64, and learning rate for both the discriminator and generator to  $1 \times 10^{-4}$ . When training the neighbour selector, we clone a copy of the trained image combiner. The learning rate is set to  $1 \times 10^{-3}$ , and the maximum training iterations is 200. When testing our augmentation against the baseline, the neighbour selector considers 20 candidates for each neighbour selection.

## 4.3 Baselines and Evaluation Protocols

Our baselines include: **1) 1-Shot+1-Query**: based on the original support set and queries; **2) 4-Shot+4-Query (Oracle)**: based on the average of four test samples for respective support set and queries; **3-5) Rotate/Affine/Color-Jitter**: based on various augmentations adopted from the Pytorch transform functions [18]. Rotate is RandomRotation with degree options from  $\{0, 180\}$ ; Affine is RandomAffine with degree options from  $\{30, 70\}$ , translate options from  $\{0.1, 0.3\}$  and scale options from  $\{0.5, 0.75\}$ ; Color-Jitter is ColorJitter with brightness, contrast and saturation as 0.2, hue as 0.1. Besides, we perform **6) Mix-Up** by augmenting each support/query sample with one additional copy. We pass 25,000 5-way-1-shot queries to test a trained FSL model under various settings. 5-way-1-shot accuracy and 95% confidence intervals are reported.

## 4.4 Overall Results

Table 1 consists of experimental results of our proposed method on the Animals dataset. Based on the results, our method can enhance Conv4-based FSL model performance by around 4% on average.



Figure 4: Illustration of the effect of neighbour selector. The first row are the original test samples, the second row are neighbours picked by either neighbour selector or inverse neighbour selector. The third row are new test samples generated by the image combiner.

## 5 Further Discussions and Ablation Studies

**Without Neighbour Selector?** To study the importance of our neighbour selector, we first visualize the neighbours and generations rendered by an *inverse neighbour selector* and the original neighbour selector. To recap, the neighbour selector sorts a set of candidate neighbours from good to bad, and returns the first  $k$  copies of the candidate neighbour samples for the actual image generation. The inverse neighbour selector is the same as the neighbour selector, except that it returns the  $k$  samples deemed to be the worst. The contrast is presented in Figure 4, which demonstrates that the neighbour selector can improve the quality of generation. This observation is further confirmed when we test the same FSL model on augmented copies returned by the inverse neighbour selector or random neighbour selector, which downgrades the ProtoNet performance on Animals dataset from around 54% to around 51% for inverse or random neighbour selector with image combiner. In this study, we set the number of neighbour candidates to consider for each generation to 10. Additionally, we observe that the higher the value, the more salient the effect of neighbour selector in general.

**Limitations and Failure Cases.** As illustrated in Figure 5, image combiner suffers from some failure cases. Furthermore, it is computationally expensive to train, taking about 2 weeks to complete the training on 8 32GB V100 GPUs. Additionally, there can be extra inference overhead in terms of both time and computation. Lastly, in some datasets with fewer similar training samples, when the neighbour selector cannot find a suitable neighbour, it has to skip the augmentation.

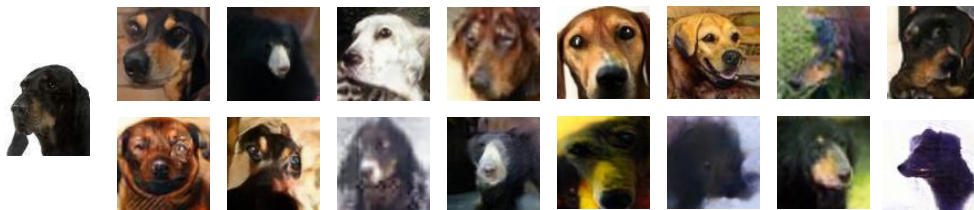


Figure 5: Image combiner failure cases.

## 6 Conclusions

Overall, in this work, we propose a method for improving the performance of trained FSL model through test-time augmentation, different from prior works that focus on training augmentation. During the test-time augmentation, an adversarial-auto-encoder-based image combiner converts training samples to test classes, improving a trained FSL model without costing extra dataset or training of the model itself.

## References

- [1] A.-N. Ciubotaru, A. Devos, B. Bozorgtabar, J.-P. Thiran, and M. Gabrani, *Revisiting few-shot learning for facial expression recognition*, 2019. arXiv: 1912.02751 [cs.CV].
- [2] G. S. Dhillon, P. Chaudhari, A. Ravichandran, and S. Soatto, “A baseline for few-shot image classification,” *arXiv preprint arXiv:1909.02729*, 2019.
- [3] L. Fe-Fei *et al.*, “A bayesian approach to unsupervised one-shot learning of object categories,” in *proceedings ninth IEEE international conference on computer vision*, IEEE, 2003, pp. 1134–1141.
- [4] H. Gao, Z. Shou, A. Zareian, H. Zhang, and S.-F. Chang, “Low-shot learning via covariance-preserving adversarial augmentation networks,” *Advances in Neural Information Processing Systems*, vol. 31, 2018.
- [5] B. Hariharan and R. Girshick, “Low-shot visual recognition by shrinking and hallucinating features,” in *Proceedings of the IEEE international conference on computer vision*, 2017, pp. 3018–3027.
- [6] K. He, X. Zhang, S. Ren, and J. Sun, “Deep residual learning for image recognition,” in *Proceedings of the IEEE conference on computer vision and pattern recognition*, 2016, pp. 770–778.
- [7] X. Huang and S. Belongie, “Arbitrary style transfer in real-time with adaptive instance normalization,” in *Proceedings of the IEEE international conference on computer vision*, 2017, pp. 1501–1510.
- [8] T. Karras, S. Laine, and T. Aila, “A style-based generator architecture for generative adversarial networks,” in *Proceedings of the IEEE/CVF conference on computer vision and pattern recognition*, 2019, pp. 4401–4410.
- [9] J. Kim, T.-H. Oh, S. Lee, F. Pan, and I. S. Kweon, “Variational prototyping-encoder: One-shot learning with prototypical images,” in *Proceedings of the IEEE/CVF Conference on Computer Vision and Pattern Recognition*, 2019, pp. 9462–9470.
- [10] Y. Kim, J. Oh, S. Kim, and S.-Y. Yun, *How to fine-tune models with few samples: Update, data augmentation, and test-time augmentation*, 2022. arXiv: 2205.07874 [cs.LG].
- [11] M.-Y. Liu, T. Breuel, and J. Kautz, “Unsupervised image-to-image translation networks,” *Advances in neural information processing systems*, vol. 30, 2017.
- [12] M.-Y. Liu *et al.*, “Few-shot unsupervised image-to-image translation,” in *arxiv*, 2019.
- [13] M.-Y. Liu *et al.*, *Few-shot unsupervised image-to-image translation*, 2019. arXiv: 1905.01723 [cs.CV].
- [14] G. Marcus, “Deep learning: A critical appraisal,” *arXiv preprint arXiv:1801.00631*, 2018.
- [15] A. Mishra, S. Krishna Reddy, A. Mittal, and H. A. Murthy, “A generative model for zero shot learning using conditional variational autoencoders,” in *Proceedings of the IEEE conference on computer vision and pattern recognition workshops*, 2018, pp. 2188–2196.
- [16] A. Oussidi and A. Elhassouny, “Deep generative models: Survey,” in *2018 International conference on intelligent systems and computer vision (ISCV)*, IEEE, 2018, pp. 1–8.
- [17] T. Park, M.-Y. Liu, T.-C. Wang, and J.-Y. Zhu, “Semantic image synthesis with spatially-adaptive normalization,” in *Proceedings of the IEEE/CVF conference on computer vision and pattern recognition*, 2019, pp. 2337–2346.
- [18] A. Paszke *et al.*, “Pytorch: An imperative style, high-performance deep learning library,” in *Advances in Neural Information Processing Systems 32*, Curran Associates, Inc., 2019, pp. 8024–8035. [Online]. Available: <http://papers.nips.cc/paper/9015-pytorch-an-imperative-style-high-performance-deep-learning-library.pdf>.
- [19] M. T. Ribeiro, S. Singh, and C. Guestrin, “Model-agnostic interpretability of machine learning,” *arXiv preprint arXiv:1606.05386*, 2016.
- [20] O. Russakovsky *et al.*, “ImageNet Large Scale Visual Recognition Challenge,” *International Journal of Computer Vision (IJCV)*, vol. 115, no. 3, pp. 211–252, 2015. DOI: 10.1007/s11263-015-0816-y.
- [21] K. Saito, K. Saenko, and M.-Y. Liu, “Coco-funit: Few-shot unsupervised image translation with a content conditioned style encoder,” in *Computer Vision—ECCV 2020: 16th European Conference, Glasgow, UK, August 23–28, 2020, Proceedings, Part III 16*, Springer, 2020, pp. 382–398.



- [22] E. Schwartz *et al.*, “Delta-encoder: An effective sample synthesis method for few-shot object recognition,” *Advances in neural information processing systems*, vol. 31, 2018.
- [23] J. Snell, K. Swersky, and R. Zemel, “Prototypical networks for few-shot learning,” *Advances in neural information processing systems*, vol. 30, 2017.
- [24] F. Sung, Y. Yang, L. Zhang, T. Xiang, P. H. Torr, and T. M. Hospedales, “Learning to compare: Relation network for few-shot learning,” in *Proceedings of the IEEE Conference on Computer Vision and Pattern Recognition*, 2018.
- [25] A. Vaswani *et al.*, *Attention is all you need*, 2017. arXiv: 1706.03762 [cs.CL].
- [26] V. K. Verma, G. Arora, A. Mishra, and P. Rai, “Generalized zero-shot learning via synthesized examples,” in *Proceedings of the IEEE conference on computer vision and pattern recognition*, 2018, pp. 4281–4289.
- [27] O. Vinyals, C. Blundell, T. Lillicrap, K. Kavukcuoglu, and D. Wierstra, *Matching networks for one shot learning*, 2016. DOI: 10.48550/ARXIV.1606.04080. [Online]. Available: <https://arxiv.org/abs/1606.04080>.
- [28] G. Wang, W. Li, M. Aertsen, J. Depreest, S. Ourselin, and T. Vercauteren, “Test-time augmentation with uncertainty estimation for deep learning-based medical image segmentation,” 2022.
- [29] K. Wang, C. Gou, Y. Duan, Y. Lin, X. Zheng, and F.-Y. Wang, “Generative adversarial networks: Introduction and outlook,” *IEEE/CAA Journal of Automatica Sinica*, vol. 4, no. 4, pp. 588–598, 2017.
- [30] T.-C. Wang, M.-Y. Liu, J.-Y. Zhu, A. Tao, J. Kautz, and B. Catanzaro, “High-resolution image synthesis and semantic manipulation with conditional gans,” in *Proceedings of the IEEE conference on computer vision and pattern recognition*, 2018, pp. 8798–8807.
- [31] Y.-X. Wang, R. Girshick, M. Hebert, and B. Hariharan, “Low-shot learning from imaginary data,” in *Proceedings of the IEEE conference on computer vision and pattern recognition*, 2018, pp. 7278–7286.
- [32] Y. Wang, Q. Yao, J. T. Kwok, and L. M. Ni, “Generalizing from a few examples: A survey on few-shot learning,” *ACM computing surveys (csur)*, vol. 53, no. 3, pp. 1–34, 2020.
- [33] S. E. Whang, Y. Roh, H. Song, and J.-G. Lee, “Data collection and quality challenges in deep learning: A data-centric ai perspective,” *The VLDB Journal*, vol. 32, no. 4, pp. 791–813, 2023.
- [34] K. Yamada and S. Matsumi, “One-shot image learning using test-time augmentation,” in *Asian Conference on Pattern Recognition*, Springer, 2021, pp. 3–16.
- [35] H.-J. Ye, H. Hu, D.-C. Zhan, and F. Sha, “Few-shot learning via embedding adaptation with set-to-set functions,” in *IEEE/CVF Conference on Computer Vision and Pattern Recognition (CVPR)*, 2020, pp. 8808–8817.
- [36] F. Yu, A. Seff, Y. Zhang, S. Song, T. Funkhouser, and J. Xiao, “Lsun: Construction of a large-scale image dataset using deep learning with humans in the loop,” *arXiv preprint arXiv:1506.03365*, 2015.
- [37] J.-Y. Zhu, T. Park, P. Isola, and A. A. Efros, “Unpaired image-to-image translation using cycle-consistent adversarial networks,” in *Proceedings of the IEEE international conference on computer vision*, 2017, pp. 2223–2232.